

## **Conversion of ethanol to light olefins over HZSM-5 type zeolites containing alkaline earth metals**

Daisuke Goto<sup>a</sup>, Yasumitsu Harada<sup>a</sup>, Yoshiyasu Furumoto<sup>a</sup>, Atsushi Taklahashi<sup>b</sup>, Tadahiro Fujitani<sup>b</sup>, Takuji Ikeda<sup>c</sup>, Yasunori Oumi<sup>a</sup>, Masahiro Sadakane<sup>a</sup>, Tsuneji Sano<sup>a,\*</sup>

<sup>a</sup> Department of Applied Chemistry, Graduate School of Engineering, Hiroshima University, Higashi-Hiroshima 739-8527, Japan

<sup>b</sup> Research Institute for Innovation in Sustainable Chemistry, National Institute of Advanced Industrial Science and Technology, Tsukuba, Ibaraki 305-8569, Japan

<sup>c</sup> Research Center for Compact Chemical Process, National Institute of Advanced Industrial Science and Technology, Tohoku, Sendai 983-8551, Japan

\*Corresponding author: Fax: +81-82-424-5494, Tel: +81-82-424-7607, E-mail: [tsano@hiroshima-u.ac.jp](mailto:tsano@hiroshima-u.ac.jp)

### **Abstract**

Protonated ZSM-5 type zeolites containing alkaline earth metals (M-HZSM-5, M: alkaline earth metal) were prepared under various synthesis conditions and their catalytic performance in conversion of ethanol to light olefins was investigated in detail. Among M-HZSM-5, Sr-HZSM-5 exhibited an excellent performance.

**Keywords:** Ethanol, ZSM-5, propylene, alkaline earth metal,

## 1. Introduction

Light olefins such as ethylene and propylene are essential raw materials for the petrochemical industry. In recent years, the demand for propylene is growing much faster than that for ethylene because of higher needs for propylene derivatives such propylene oxide and polypropylene. Propylene is mainly produced as co-product of ethylene by steam cracking of naphtha. From the viewpoints of the increase in the oil price and environmental protection, recently, the development of other routes for propylene production, especially from bio-ethanol obtained fermentation of biomass has attracted much attention. The production of light olefins from bio-ethanol, renewable biomass, is an example of the carbon neutral process. However, there are only few reports concerning production of light olefins, especially propylene from ethanol [1-5]. The conversion process using zeolite catalysts is considered to be similar to that of methanol conversion. However, the catalytic activity and the stability of catalysts are insufficient for industrial processes.

We already investigated the production of light olefins from methanol and developed excellent HZSM-5 catalysts containing alkaline earth metals (M-HZSM-5, M: alkaline earth metal), which showed the high yields of ethylene and propylene more than 60% and had a long catalysts life over 2,000 h [6]. In this study, therefore, we investigated the potential of M-HZSM-5 for ethanol conversion to light olefins in detail.

## 2. Experimental

### 2.1 Synthesis of HZSM-5 zeolites containing alkaline earth metals

ZSM-5 type zeolites containing alkaline earth metals (M-HZSM-5, M: alkaline earth metal) were synthesized as follows. Certain amounts of aluminum nitrate, colloidal silica ( $\text{SiO}_2=30.5$  wt%,  $\text{Na}_2\text{O}=0.4$  wt%,  $\text{H}_2\text{O}=69.1$  wt%, Cataloid SI-30, Catalysts & Chemicals Ind. Co. Ltd., Japan) and tetrapropylammonium bromide (TPABr, Tokyo Chemical Ind. Co. Ltd., Japan)

were added to a stirred mixture of alkaline earth metal acetate and sodium hydroxide in deionized water. The hydrogel composition was:  $\text{SiO}_2/\text{Al}_2\text{O}_3=40-600$ ,  $\text{OH}^-/\text{SiO}_2=0.1-0.2$ ,  $\text{TPABr}/\text{SiO}_2=0.1$ ,  $\text{H}_2\text{O}/\text{SiO}_2=40$  and  $\text{M}/\text{Al}=0.5-2.5$ . The resultant hydrogel was transferred into a 300 ml stainless-steel autoclave and stirred at  $160^\circ\text{C}$  under autogenous pressure for 16 h. The precipitated crystals obtained were washed with deionized water, dried at  $120^\circ\text{C}$  for one night, and calcined at  $500^\circ\text{C}$  for 20 h to remove the organic cations occluded into zeolite framework. The zeolite was protonated in a  $0.6 \text{ mol dm}^{-3}$  hydrochloric acid solution at room temperature for 24 h, and calcined in air at  $500^\circ\text{C}$  for 8 h.

## 2.2 Characterization

The X-ray diffraction (XRD) patterns of the solid products were collected using a powder X-ray diffractometer (Bruker, D8 Advance) with graphite monochromatized  $\text{Cu K}\alpha$  radiation at 40 kV and 30 mA. Si/Al ratios were determined by X-ray fluorescence (XRF, Philips PW 2400). 0.5 g of a sample was fused with 5 g of dilithium tetraborate ( $\text{Li}_2\text{B}_4\text{O}_7$ ) at  $1100^\circ\text{C}$ . The crystal morphology was observed by scanning electron microscopy (SEM, JEOL JSM-6320FS). The thermal analysis was carried out using a TG/DTA apparatus (SSC/5200 Seiko Instruments). The sample ca. 7 mg was heated in a flow of air ( $50 \text{ mL min}^{-1}$ ) at  $10^\circ\text{C min}^{-1}$  from room temperature to  $800^\circ\text{C}$ .  $^{27}\text{Al}$  MAS NMR spectra were recorded using a 7 mm diameter zirconia rotor on Bruker Avance DRX-400 at 100.6 MHz, 104.3 MHz and 79.5 MHz, respectively. The rotor was spun at 6 kHz. The spectra were accumulated with  $2.3 \mu\text{s}$  pulses, 1 s recycle delay and 4000 scans.  $\text{Al}(\text{NO}_3)_3 \cdot 9\text{H}_2\text{O}$  was used as chemical shift. Prior to  $^{27}\text{Al}$  MAS NMR measurement, the sample was moisture-equilibrated over a saturated solution of  $\text{NH}_4\text{Cl}$  for 24 h. Nitrogen adsorption isotherms at  $-196^\circ\text{C}$  were performed using a conventional volumetric apparatus (Bel Japan, BELSORP 28SA). Prior to adsorption measurements, the calcined samples (ca. 0.1 g) were evacuated at  $400^\circ\text{C}$  for 10 h. The IR spectra were recorded

on a FT-IR spectrometer (JEOL JIR-7000) with a resolution of  $4\text{ cm}^{-1}$  at room temperature. For OH groups stretching region measurements, the sample was pressed into a self-supporting thin wafer (ca.  $6.4\text{ mg cm}^{-2}$ ) and placed into a quartz IR cell equipped with  $\text{CaF}_2$  windows. Prior to measurement, each sample was dehydrated under vacuum at  $400\text{ }^\circ\text{C}$  for 2 h. The acidity and distribution of zeolites were measured by the temperature programmed desorption of ammonia ( $\text{NH}_3$ -TPD with a CAT-B-82  $\text{NH}_3$ -TPD apparatus (Bel Jpn). Helium was used as a carrier gas. The temperature range was 100 to  $600^\circ\text{C}$  with the heating rate of  $10^\circ\text{C}/\text{min}$ .

### 2.3 Ethanol conversion

Ethanol conversion was carried out at  $400\text{-}600\text{ }^\circ\text{C}$  and  $\text{W/F}=4\text{ h}^{-1}$  in an atmospheric pressure flow system. A certain amount of zeolite (14-28 mesh) was retained by quartz wool at the center of a quartz reactor of a 10 mm inner diameter. A thermocouple reaching into the center of the catalysts bed was used to measure the temperature during the reaction. The catalysts were activated at  $500^\circ\text{C}$  for 1 h in flowing nitrogen before reaction. Ethanol (>99.5%, Wako Chem., Japan) was pumped into the vaporizer and mixed with  $\text{N}_2$  at a total flow rate of  $\&\&\&\text{ ml/min}$  ( $\text{C}_2\text{H}_5\text{OH}:\text{N}_2=50/50\text{ mol}\%$ ). The products obtained were analyzed on-line with gas chromatographs (Shimadzu GC-14) equipped with a TCD and FID type detectors. An InertCap 1701 and Gasukuropack-54 columns were used.

## 3. Results and discussion

### 3.1. Ethanol conversion over HZSM-5

At first, in order to clarify a difference in reaction behavior between methanol conversion and ethanol conversion, HZSM-5 zeolites with various  $\text{SiO}_2/\text{Al}_2\text{O}_3$  ratios were prepared and subjected to ethanol conversion reaction. As listed in Table 1, the BET surface area of HZSM-5 zeolite obtained were larger than  $300\text{ m}^2/\text{g}$  and the crystal size was  $0.1\text{-}6.0\text{ }\mu\text{m}$ . Figure 1 shows the relationship between  $\text{SiO}_2/\text{Al}_2\text{O}_3$  ratio and the light olefin yields at the

reaction conditions of Temp.=500 °C and W/F=0.0025 g/ml.min. The propylene yield increased with a decrease in the SiO<sub>2</sub>/Al<sub>2</sub>O<sub>3</sub> ratio and reached the maximum value (ca. 27 %) at the SiO<sub>2</sub>/Al<sub>2</sub>O<sub>3</sub> ratio of 50, while the ethylene yield dramatically decreased with a decrease in the SiO<sub>2</sub>/Al<sub>2</sub>O<sub>3</sub> ratios. The relationship between the SiO<sub>2</sub>/Al<sub>2</sub>O<sub>3</sub> ratio and the light olefin yield was considerably different from that observed in the methanol conversion, in which ethylene and propylene were more effectively produced on the siliceous zeolites. Namely, oligomerization of ethylene produced by dehydration of ethanol hardly occurs on siliceous HZSM-5 due to lower Brønsted acid sites, suggesting that aluminous zeolite is suitable for the ethanol conversion to light olefins. Taking into account that light olefins such as propylene are produced by cracking of higher olefins, however, it is reasonable to consider that the product distribution is strongly dependent upon the contact time. Therefore, the influence of W/F on the product distribution of ethanol conversion over HZSM-5 zeolites with SiO<sub>2</sub>/Al<sub>2</sub>O<sub>3</sub> ratio of 76 and 184 were investigated. As can be seen in Fig.2, the higher C<sub>3</sub>H<sub>6</sub> yield was obtained at higher W/F. Namely, the C<sub>3</sub>H<sub>6</sub> yield is strongly affected by the W/F.

As water is produced in the ethanol conversion, the zeolite catalyst is exposed to a moisture-rich atmosphere during the reaction. Dealumination from zeolite framework is accelerated in a moisture-rich atmosphere at high temperatures, resulting in the serious deactivation of zeolite catalyst because of structural degradation of zeolite. Therefore, the stability of acid sites in HZSM-5 zeolite should be also investigated. Fig. 3 shows the C<sub>3</sub>H<sub>6</sub> yield evolution with time on stream over HZSM-5 zeolite with SiO<sub>2</sub>/Al<sub>2</sub>O<sub>3</sub> ratio of 52 and 184. To keep the initial C<sub>3</sub>H<sub>6</sub> yield constant, the W/F values were set to be 0.125g/ml/min for HZSM-5 with SiO<sub>2</sub>/Al<sub>2</sub>O<sub>3</sub> ratio of 52 and 0.03 g/ml/min for HZSM-5 with 184. As can be seen in Fig. 3, The C<sub>3</sub>H<sub>6</sub> yield for HZSM-5 with SiO<sub>2</sub>/Al<sub>2</sub>O<sub>3</sub> ratio of 52 gradually decreases with time on stream, while there was only a slight decrease was observed. To clarify the

difference, the amount of framework aluminium was measured by  $^{27}\text{Al}$  MAS NMR. Figure 4 shows the  $^{27}\text{Al}$  MAS NMR spectra of HZSM-5 zeolite with  $\text{SiO}_2/\text{Al}_2\text{O}_3$  ratio of 52 and 186 before and after the reaction. In all spectra, the peak assigned to tetrahedrally coordinated framework aluminium was observed at ca. 54 ppm. However, there was a large difference in the degree of dealumination, namely HZSM-5 with  $\text{SiO}_2/\text{Al}_2\text{O}_3$  ratio of 52 exhibited the higher dealumination. From a standpoint of the stability of acid sites against steaming, the above results indicate that the siliceous HZSM-5 zeolite is suitable for the ethanol conversion to light olefins. Therefore, we tried to develop HZSM-5 zeolite catalyst from a standpoint of improving the steam stability of zeolite in the following experiments. This is consistent with our previous results of dealumination of HZSM-5 by steaming [7,8]. The dealumination rate has an apparent third-order dependence on the number of framework aluminums. As the framework atoms are isolated from each other in the case of highly siliceous zeolites such as ZSM-5, this indicates that the dealumination via hydrolysis of Si-O-Al bonds in the zeolite framework is catalysed by acid (Protons) which move freely in the zeolite pores. Therefore, we have the potential of catalytic activity of HZSM-5 zeolites modified with alkaline earth metals

### **3.2. Ethanol conversion over M-HZSM-5**

Table 2 lists the hydrothermal synthesis conditions and the characteristics of various M-HZSM-5 prepared. The prepared M-HZSM-5 had a well-defined MFI type zeolite structure, as demonstrated by their XRD patterns (Fig. 5). There were no diffraction peaks other than those of ZSM-5. The BET surface area measured by  $\text{N}_2$  adsorption was larger than  $300 \text{ m}^2/\text{g}$  and was the same as that of HZSM zeolite. The typical SEM images of various M-HZSM-5 were also shown in Fig. 5. The M/Al ratio in M-HZSM-5 was changed from 0.1 to 0.5.

Considering that the high reaction temperature above 500°C favor for production of light olefins, and that experiments using C<sub>2</sub>C<sub>4</sub>olefins as the feed instead of ethanol showed cracking of the olefins to be predominant and aromatization of the olefins to be suppressed at high temperatures, we applied M-HZSM-5 to the ethanol conversion. M-HZSM-5 are capable of operating at high temperatures due to the weak acidity and shows the excellent catalytic performance for methanol conversion to light olefins [3]. Fig.5 shows the relationship between the M/Al ratio and the C<sub>3</sub>H<sub>6</sub> yield. Except for Mg-HZSM-5, the C<sub>3</sub>H<sub>6</sub> yield increased with an increase in the M/Al ratio and reached at the maximum value at the M/Al ratio of 0.1. Among M-HZSM-5, Sr-HZSM-5 showed the highest C<sub>3</sub>H<sub>6</sub> yield. The further increase in the M/Al ratio caused the decrease in the C<sub>3</sub>H<sub>6</sub> yield. As shown in Figure 6, the decrease in the C<sub>3</sub>H<sub>6</sub> yield was due to a considerable increase in the C<sub>2</sub>H<sub>4</sub> yield. This indicates a suppression of oligomerization of ethylene over strong acid sites modification with alkaline earth metals. The decrease in the number of strong acid sites was confirmed from NH<sub>3</sub>-TPD measurements that the intensity of peak

To clarify the chemical state of aluminums in the M-HZSM-5, the <sup>27</sup>Al MAS NMR spectra were measured. Fig. 3(A) shows the typical <sup>27</sup>Al MAS NMR spectra of various M-HZSM-5. Only a sharp peak at ca. 54 ppm was observed in all spectra, which is a characteristic resonance of tetrahedrally coordinated framework aluminums [11]. No peak assigned to non-framework aluminums (extraframework aluminums) was observed around 0 ppm. Therefore, it was clearly revealed that all of aluminums in the M-HZSM-5 are present in the zeolitic framework.

The presence of  $\text{TMA}^+$  cation in the cages was further confirmed by the preliminary Rietveld refinement based on powder XRD data. The structure refinement was carried out by using program RIETAN-FP [18]. Distribution of extraframework atoms was estimated by the maximum entropy method using a program PRIMA [19]. The refined structural model was visualized by a program VESTA [20]. The model shows that free-rotational  $\text{TMA}^+$  cation is present in hexakaidecahedra  $5^{12}6^4$  cages as depicted in Figure 6. Furthermore, a small amount of electron densities was observed in the center of another  $5^{12}$  cages from MEM density maps, indicating the presence of adsorbed water molecule or some hydrocarbon species. However,  $(\text{CH}_3)_3\text{NH}^+$  cation was hardly observed in the refinement, suggesting that a small amount of  $(\text{CH}_3)_3\text{NH}^+$  cation observed in  $^{13}\text{C}$  CP/MAS NMR spectrum may be located disorderly in  $5^{12}6^4$  or  $5^{12}$  cages.

#### **4. Conclusions**

From all of above results, it was found that the crystal size of M-HZSM-5 can be easily controlled by addition of  $\text{H}_3\text{BO}_3$  and the dealumination by steaming is greatly depressed by adding alkaline earth metal. The high hydrothermal stability of M-HZSM-5 was also confirmed from methanol conversion on the steamed zeolites. Ca- and Sr-HZSM-5 showed the high selectivity to light olefins even after steaming at 600 °C for 7 days.



## Acknowledgement

This work was supported by a New Energy and Industrial Technology Development Organization (NEDO) grant.

## References

- [1] H. Oikawa, Y. Shibata, K. Inazu, Y. Iwase, K. Murai, S. Hyodo, G. Kobayashi, T. Baba, *Appl. Catal. A* 312 (2006) 181-185.
- [2] K. Murata, M. Inaba, T. Takahara, *J. Jpn. Petrol. Inst.* 51 (2008) 234-239.
- [3] Q. Zhu, J.N. Kondo, S. Inagakli, T. Tatsumi, *Top. Catal.* 52 (2009) 1272-1280.
- [4] T. Yamazaki, N. Kikuchi, M. Katoh, Y. Okada, T. Yoshikawa, M. Wada, *J. Jpn. Petrol. Inst.* 52 (2009) 234-247.
- [5] Z. Song, A. Takahashi, N. Mimura, T. Fujitani, *Catal. Lett.* 131 (2009) 364-369.
- [6] T. Sano, Y. Kiyozumi, S. Shin, *J. Jpn. Petrol. Inst.* 35 (1992) 429-440.
- [7] T. Sano, K. Suzuki, H. Shoji, S. Ikai, K. Okabe, T. Murakami, S. Shin, H. Hagiwara, H. Takaya, *Chem. Lett.* (1987) 1421-1424.
- [8] T. Sano, N. Yamashita, Y. Iwami, K. Takeda, Y. Kawakami, *Zeolites* 16 (1996) 258-264.
- [9] M. Moraes, W.S.F. Pinto, W.A. Gonzalez, L.M.P.M. Carmo, N.M.R. Pastura, E.R. Lachter, *Appl. Catal. A* 138 (1996) L7-L12.
- [10] T. Yamaguchi, C. Nishimichi, *Catal. Today* 16 (1993) 555-562.
- [11] D. M. Antonelli, J. Y. Ying, *Angew. Chem. Int. Ed. Engl.* 35 (1996) 426-429.
- [12] P. Yang, D. Zhao, D. I. Margolese, B. F. Chmelka, G. D. Stucky, *Nature* 396 (1998)

152-155.

[13] B. Lee, D. Lu, J. N. Kondo, K. Domen, *J. Am. Chem. Soc.* 124 (2004) 11256-11257.

[14] K. Asakura, Y. Iwasa, *Chem. Lett.* (1986) 859-862.

[15] J.-M. Jehng, I.E. Wachs, *Catal. Today* 8 (1990) 37-55.

[16] T. Tanaka, H. Nojima, H. Yoshida, H. Nakagawa, T. Funabuki, S. Yoshida, *Catal. Today* 16 (1993) 297-307.

[17] F.M.T. Mendes, C.A. Perez, R.R. Soares, F.B. Noronha, M. Schmal, *Catal. Today* 78 (2003) 449-458.

[18] J.M. Jehng, I.E. Wachs, *J. Phys. Chem.* 95 (1991) 7373-7379.

[19] J.M. Jehng, I.E. Wachs, *Chem. Mater.* 3 (1991) 100-107.

[20] J.M. Jehng, I.E. Wachs, *Catal. Today* 16 (1993) 417-426.

[21] T. Tanaka, T. Yoshida, H. Yoshida, H. Aritani, T. Funabuki, S. Yoshida, J.M. Jehng, I.E. Wachs, *Catal. Today* 28 (1996) 71-78.

## Figure captions

**Fig. 1.** Conversion of EtOH to light olefins over HZSM-5 zeolites with SiO<sub>2</sub>/Al<sub>2</sub>O<sub>3</sub> ratios of 52 (●), 76 (■), and 184 (▲).  
Temp.= 500 °C.

**Fig. 2.** C<sub>3</sub>H<sub>6</sub> yield evolution with time on stream on HZSM-5 zeolites with SiO<sub>2</sub>/Al<sub>2</sub>O<sub>3</sub> ratios of 52 (○) and 186 (●).  
Reaction condition:Temp= 550 °C, W/F= 0.0125 (○) and 0.03 (●) g<sub>cat</sub>/ml/min.

**Fig. 3.** <sup>27</sup>Al MAS NMR spectra of HZSM-5 zeolites with SiO<sub>2</sub>/Al<sub>2</sub>O<sub>3</sub> ratios of 52 (a, b) and 186 (c, d) before (a, c) and after (b, d) reaction.

**Fig. 4.** XRD patterns and SEM images of (a) HZSM-5 (Sample no.6), (b) Mg-HZSM-5 (no. 9), (c) Ca-HZSM-5 (no. 11), (d) Sr-HZSM-5 (no. 15) and (e) Ba-HZSM-5 (no. 21).

**Fig. 5.** Influence of M/Al ratio of M-HZSM-5 on C<sub>3</sub>H<sub>6</sub> yield over (◆) Mg-HZSM-5, (□) Ca-HZSM-5, (○) Sr-HZSM-5, and (▲) Ba-HZSM-5.  
Reaction condition:Temp= 500 °C, W/F= 0.03 g<sub>cat</sub>/ml/min.

**Fig. 6.** Influence of Sr/Al ratio of Sr-HZSM-5 on (○) C<sub>2</sub>H<sub>4</sub>, (■) C<sub>3</sub>H<sub>6</sub> and (▲) C<sub>4</sub>H<sub>8</sub> yields.  
Reaction condition:Temp= 500 °C, W/F= 0.03 g<sub>cat</sub>/ml/min.

**Fig. 7.** NH<sub>3</sub>-TPD curves of (—) HZSM-5 (Sample no. 6), (---) Sr-HZSM-5 (no. 15) and (···) Sr-HZSM-5 (no. 17).

**Fig. 8.** C<sub>3</sub>H<sub>6</sub> yield evolution with time on stream on (●) Sr-HZSM-5 (Sample no. 15) and (○) HZSM-5 (no. 6).  
Reaction condition:Temp= 500 °C, W/F= 0.03 g<sub>cat</sub>/ml/min.

**Fig. 9.** <sup>27</sup>Al MAS NMR spectra of HZSM-5 zeolites with SiO<sub>2</sub>/Al<sub>2</sub>O<sub>3</sub> ratios of (a, b) HZSM-5 (Sample no. 2) and (c, d) Sr-HZSM-5 (no. 15) before (a, c) and after (b, d) reaction.

**Fig. 10.** Influence of W/F on C<sub>3</sub>H<sub>6</sub> yield for (●) HZSM-5 (Al), (■) HZSM-5 (Ga), and (▲)

HZSM-5 (Fe).

**Fig. 11.** Crystal Structure model of Sr-HZSM-5 ( $\text{SiO}_2/\text{Al}_2\text{O}_3 = 53$ ,  $\text{Sr}/\text{Al} = 0.58$ ).

**Fig. 12.** Fig. 12  $\text{N}_2$  adsorption isotherms on ( $\square$ ) HZSM-5 (Sample no. 6), ( $\circ$ ) Sr-HZSM-5 (no. 15) and ( $\triangle$ ) Sr-ZSM-5 (no. 17).

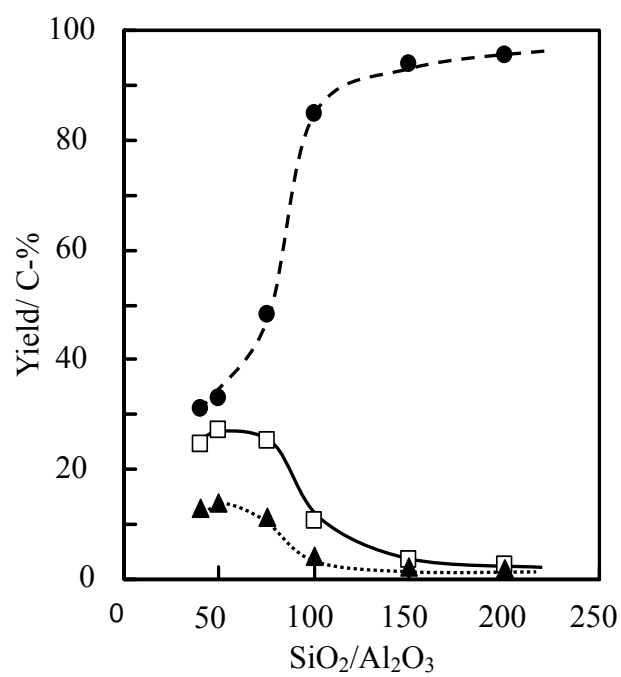


Fig. 1 Influence of SiO<sub>2</sub>/Al<sub>2</sub>O<sub>3</sub> ratio of HZSM-5 on (●) C<sub>2</sub>H<sub>4</sub>, (□) C<sub>3</sub>H<sub>6</sub> and (▲) C<sub>4</sub>H<sub>8</sub> yields.  
Reaction condition: Temp= 500 °C, W/F= 0.0025 g<sub>cat</sub>/ml/min.

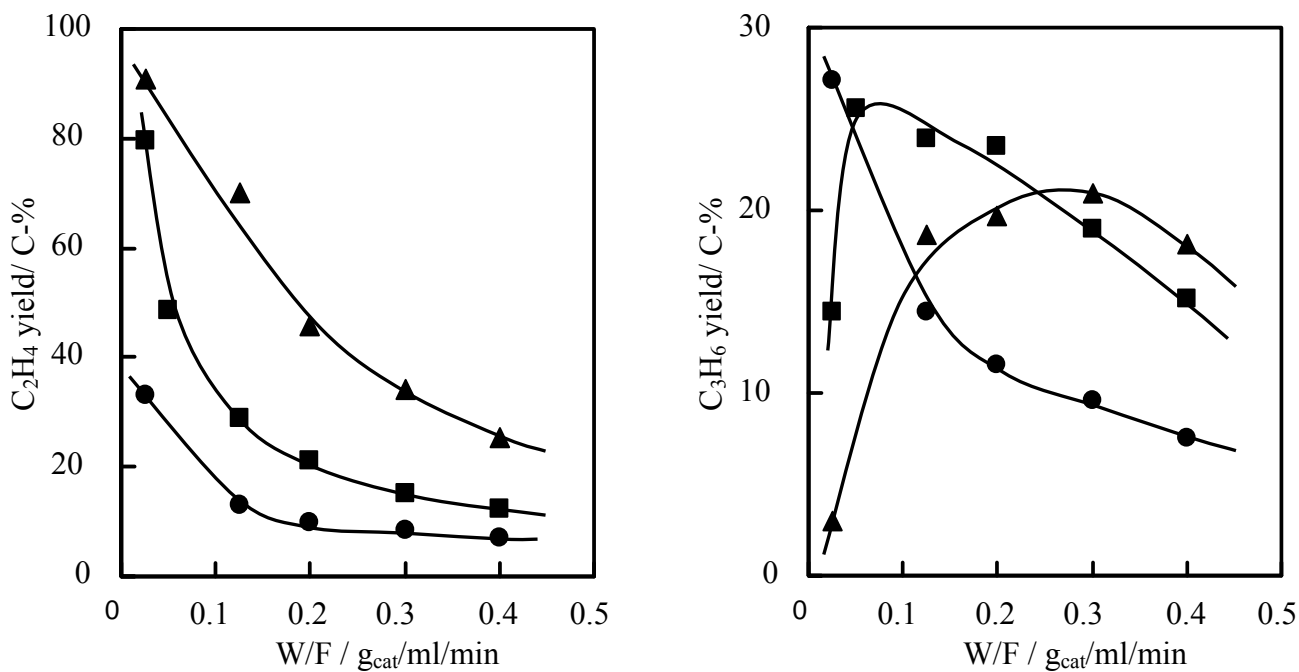


Fig. 2 Conversion of EtOH to light olefins over HZSM-5 zeolites with SiO<sub>2</sub>/Al<sub>2</sub>O<sub>3</sub> ratios of 52 (●), 76 (■), and 184 (▲). Temp.= 500 °C.

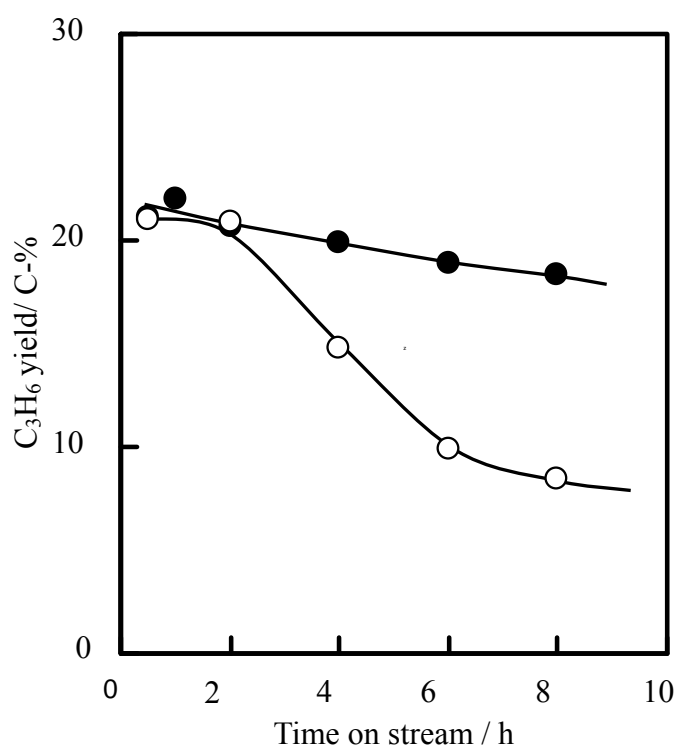


Fig. 3 C<sub>3</sub>H<sub>6</sub> yield evolution with time on stream on HZSM-5 zeolites with SiO<sub>2</sub>/Al<sub>2</sub>O<sub>3</sub> ratios of 52 (○) and 186 (●). Reaction condition: Temp= 550 °C, W/F= 0.0125 (○) and 0.03 (●) g<sub>cat</sub>/ml/min.

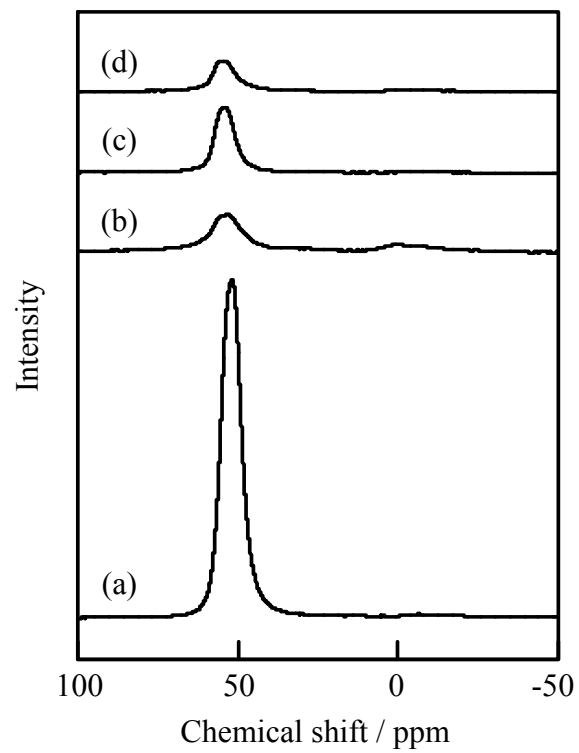


Fig. 4  $^{27}\text{Al}$  MAS NMR spectra of HZSM-5 zeolites with  $\text{SiO}_2/\text{Al}_2\text{O}_3$  ratios of 52 (a, b) and 186 (c, d) before (a, c) and after (b, d) reaction.



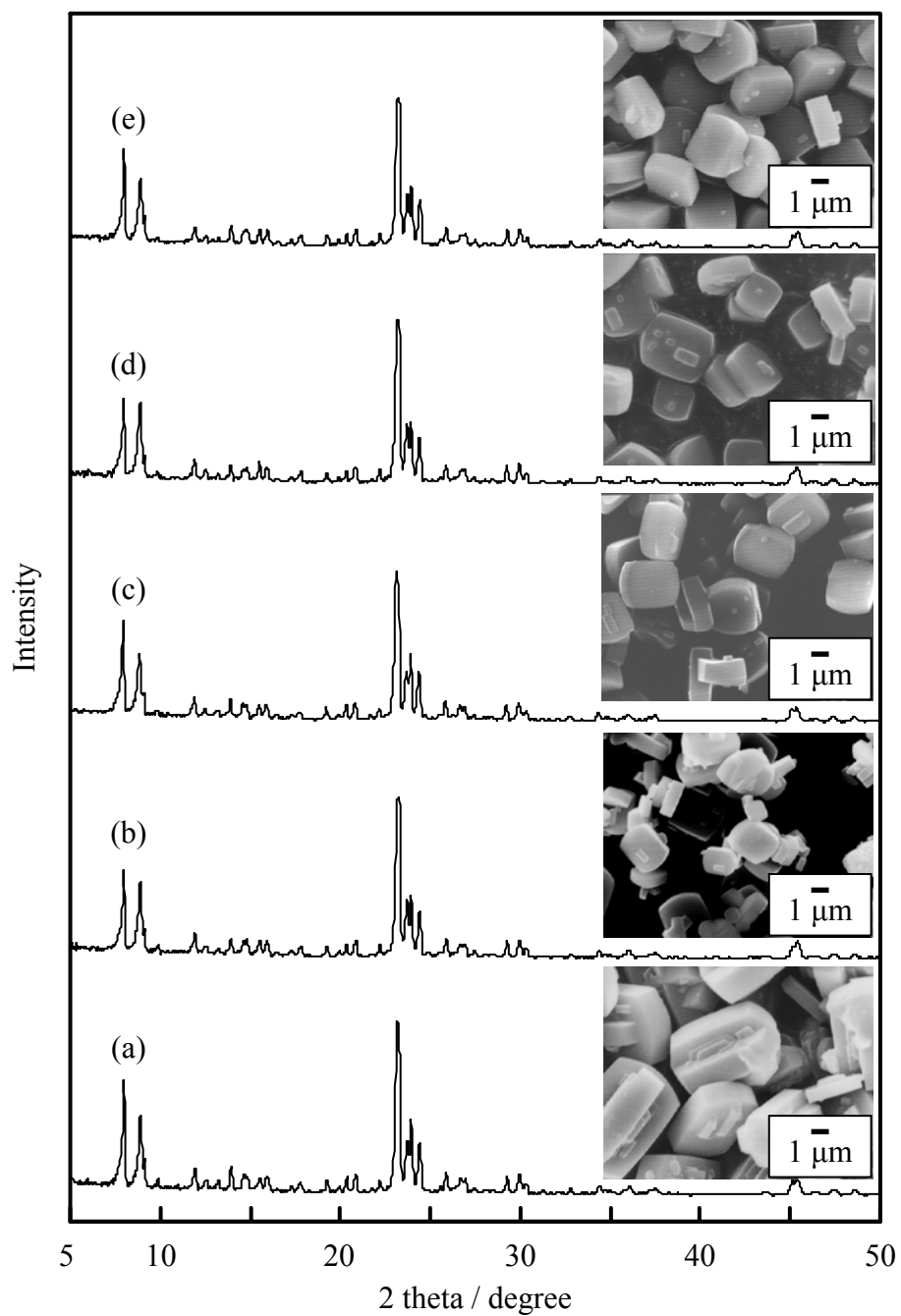


Fig. 5 XRD patterns and SEM images of (a) HZSM-5 (Sample no.6), (b) Mg-HZSM-5 (no. 9), (c) Ca-HZSM-5 (no. 11), (d) Sr-HZSM-5 (no. 15) and (e) Ba-HZSM-5 (no. 21).

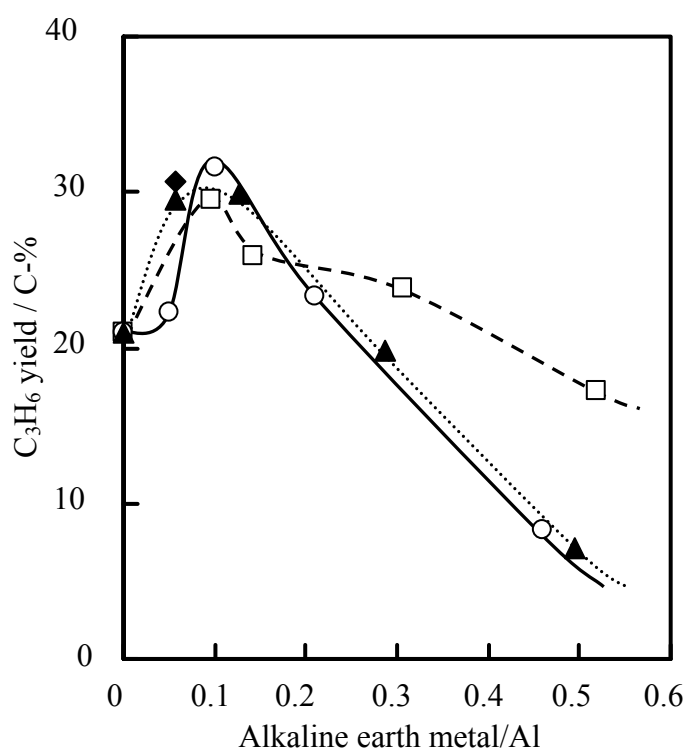


Fig. 6 Influence of M/Al ratio of M-HZSM-5 on C<sub>3</sub>H<sub>6</sub> yield over (◆) Mg-HZSM-5, (□) Ca-HZSM-5, (○) Sr-HZSM-5, and (▲) Ba-HZSM-5. Reaction condition: Temp= 500 °C, W/F= 0.03 g<sub>cat</sub>/ml/min.

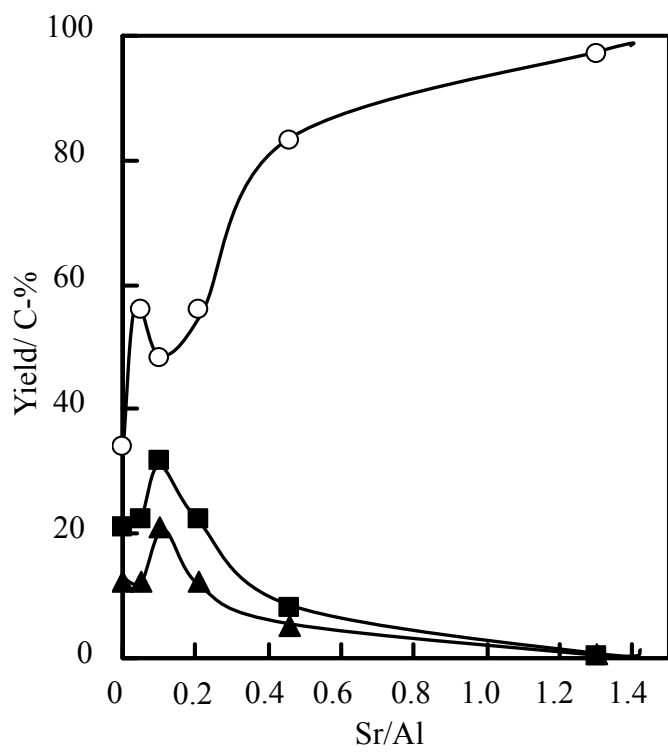


Fig. 7 Influence of Sr/Al ratio of Sr-HZSM-5 on (○) C<sub>2</sub>H<sub>4</sub>, (■) C<sub>3</sub>H<sub>6</sub> and (▲) C<sub>4</sub>H<sub>8</sub> yields.  
Reaction condition: Temp= 500 °C, W/F= 0.03 g<sub>cat</sub>/ml/min.

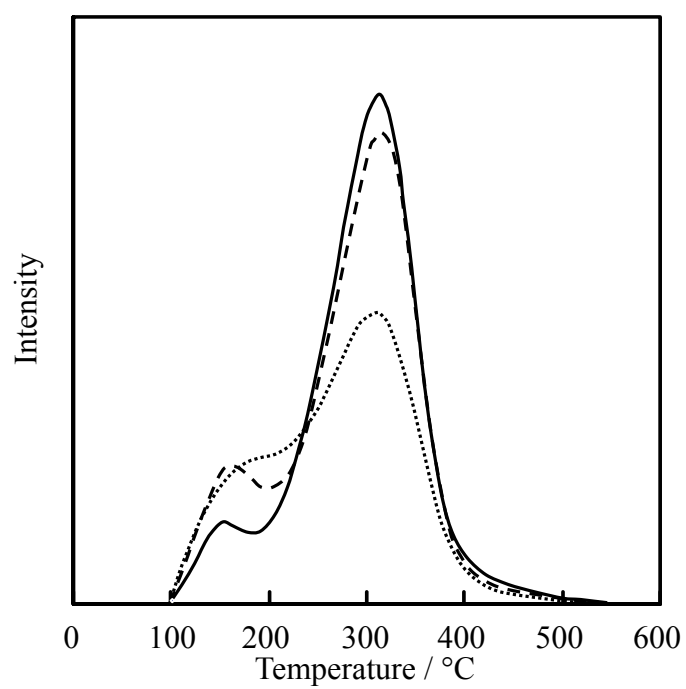


Fig. 8 NH<sub>3</sub>-TPD curves of (—) HZSM-5 (Sample no. 6), (---) Sr-HZSM-5 (no. 15) and (···) Sr-HZSM-5 (no. 17).

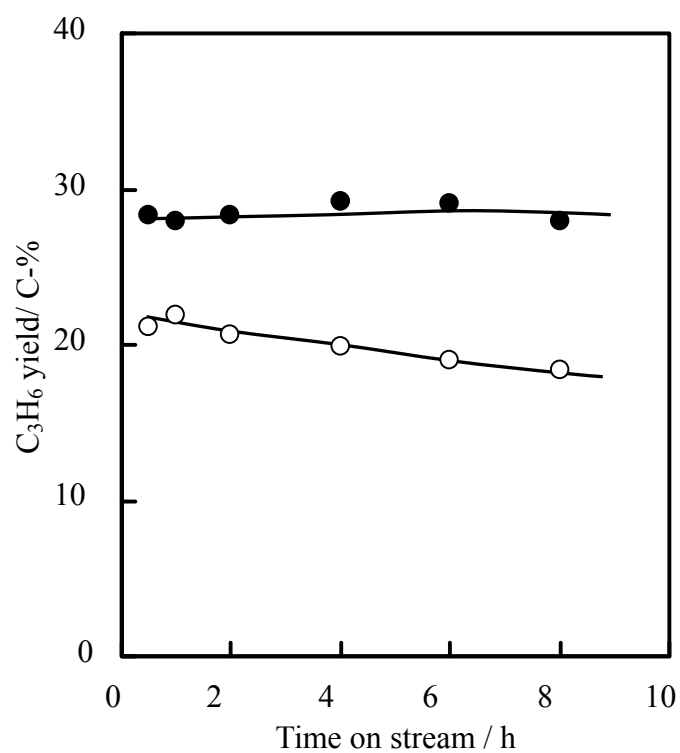


Fig. 9 C<sub>3</sub>H<sub>6</sub> yield evolution with time on stream on (●) Sr-HZSM-5 (Sample no. 15) and (○) HZSM-5 (no. 6).  
Reaction condition:Temp= 500 °C, W/F= 0.03 g<sub>cat</sub>/ml/min.

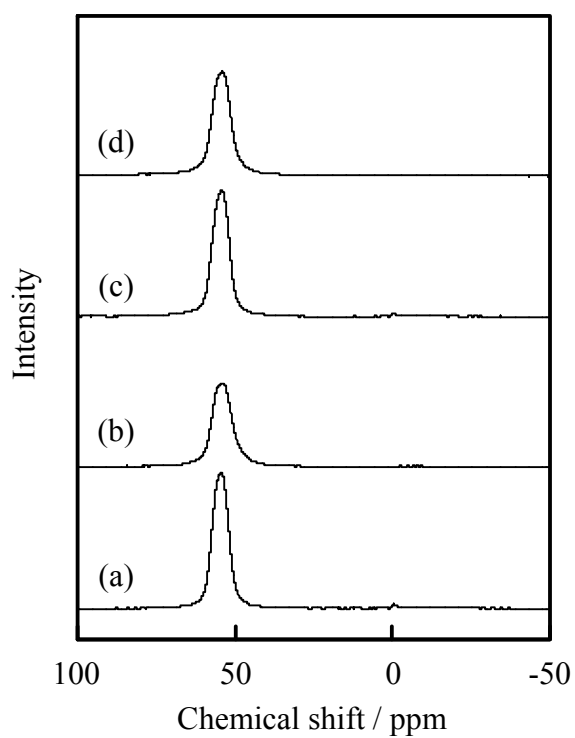


Fig. 10  $^{27}\text{Al}$  MAS NMR spectra of HZSM-5 zeolites with  $\text{SiO}_2/\text{Al}_2\text{O}_3$  ratios of (a, b) HZSM-5 (Sample no. 2) and (c, d) Sr-HZSM-5 (no. 15) before (a, c) and after (b, d) reaction.

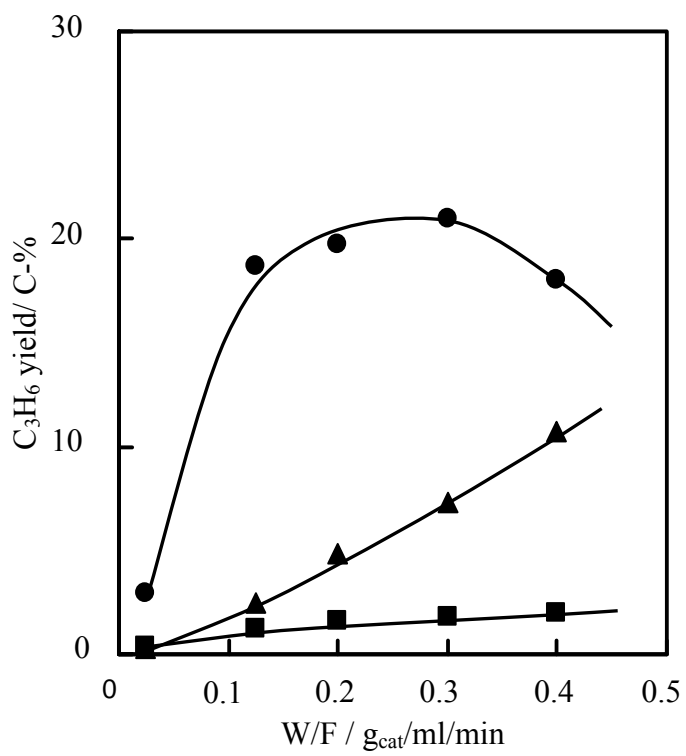


Fig. 11 Influence of W/F on C<sub>3</sub>H<sub>6</sub> yield for (●) HZSM-5 (Al), (■) HZSM-5 (Ga), and (▲) HZSM-5 (Fe).

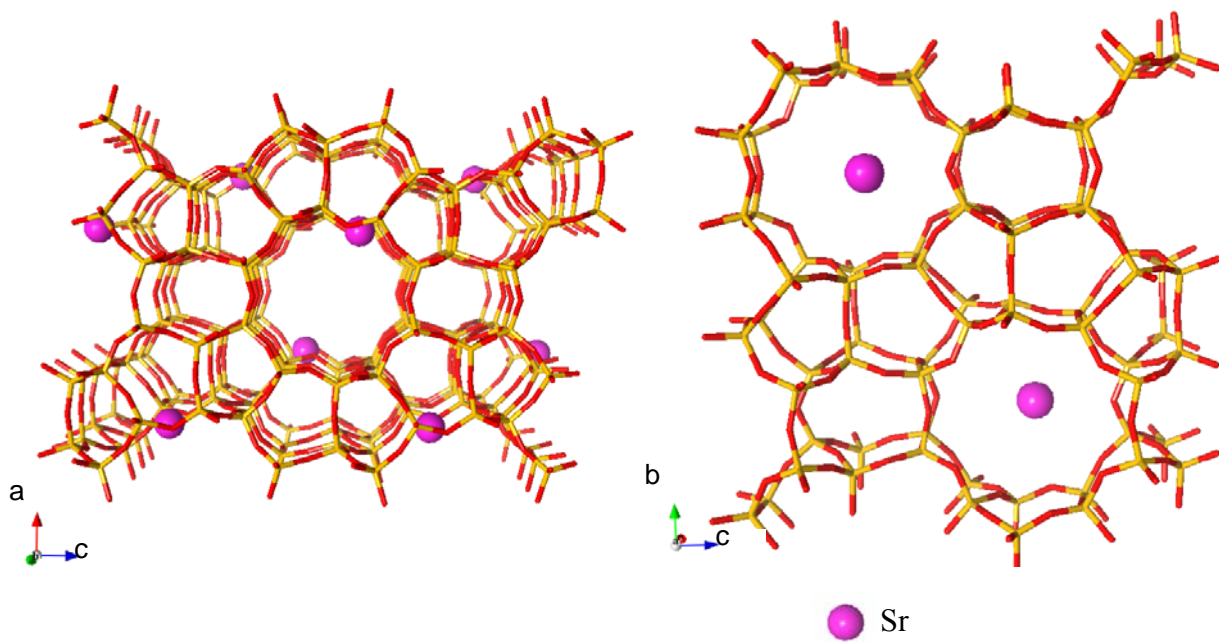


Fig. 12 Crystal Structure model of Sr-HZSM-5  
( $\text{SiO}_2/\text{Al}_2\text{O}_3 = 53$ ,  $\text{Sr}/\text{Al} = 0.58$ ).



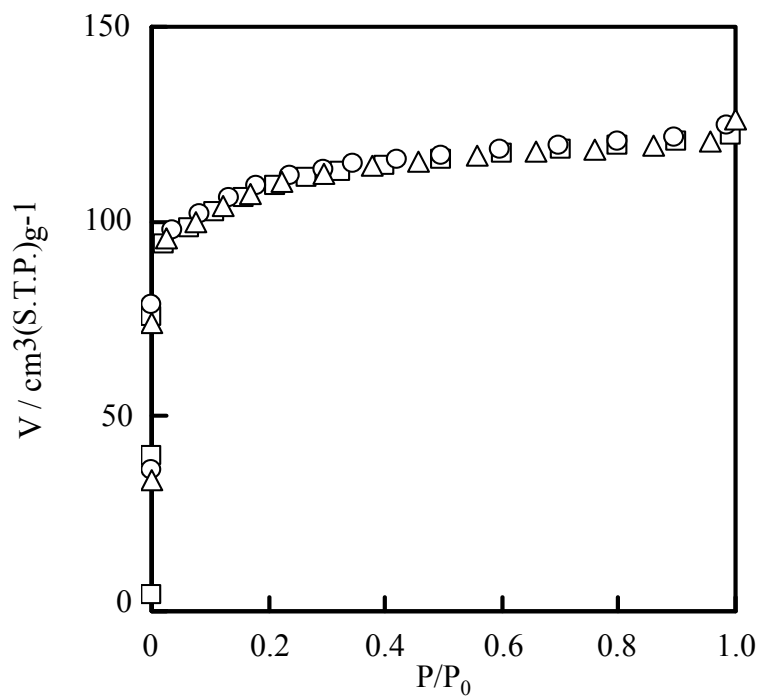


Fig. 13  $\text{N}_2$  adsorption isotherms on ( $\square$ ) HZSM-5 (Sample no. 6), ( $\circ$ ) Sr-HZSM-5 (no. 15) and ( $\triangle$ ) Sr-ZSM-5 (no. 17).

Table 1

Synthesis conditions and characteristics of HZSM-5 zeolites

Sample no.	Synthesis mixture <sup>a</sup>		Product		
	SiO <sub>2</sub> /Al <sub>2</sub> O <sub>3</sub> ratio	OH <sup>-</sup> / SiO <sub>2</sub>	SiO <sub>2</sub> /Al <sub>2</sub> O <sub>3</sub> ratio <sup>b</sup>	Surface area <sup>c</sup> (m <sup>2</sup> g <sup>-1</sup> )	Particle size (μm)
1	40	0.2	47	363	0.1-0.2
2	50	0.2	52	358	1-2
3	75	0.2	76	377	2-5
4	100	0.1	107	365	3-4
5	150	0.1	146	361	3-4
6	200	0.1	184	357	4-6
7	400	0.1	354	387	3-4
8	600	0.1	514	395	4-5

<sup>a</sup>Synthesis condition: TPABr/SiO<sub>2</sub>= 0.1, Temp.= 160 °C, Time= 16 h.<sup>b</sup>Determined by XRF.<sup>c</sup>Determined by the BET method.

Table 2

Synthesis conditions and characteristics of alkaline earth metal containing HZSM-5 zeolites (M-HZSM-5)

Sample no.	Synthesis mixture <sup>a</sup>		Product <sup>b</sup>		Surface Area <sup>c</sup> (m <sup>2</sup> g <sup>-1</sup> )	Particle size (μm)
	SiO <sub>2</sub> / Al <sub>2</sub> O <sub>3</sub> ratio	M/Al	SiO <sub>2</sub> / Al <sub>2</sub> O <sub>3</sub> <sup>a</sup> ratio	M/Al <sup>a</sup>		
9	200	0.05 (Mg)	198	0.06	371	2-3
10	200	0.05 (Ca)	206	0.10	374	2.5-3
11	200	0.125 (Ca)	200	0.14	367	3-4
12	200	0.25 (Ca)	213	0.31	373	2-5
13	200	0.50 (Ca)	202	0.52	364	3-4
14	200	0.05 (Sr)	202	0.04	377	5-10
15	200	0.125 (Sr)	203	0.10	374	3-5
16	200	0.25 (Sr)	202	0.21	368	2-3
17	200	0.50 (Sr)	211	0.46	361	6-9
18	150	0.125 (Sr)	104	0.09	354	3-5
19	100	0.125 (Sr)	153	0.10	365	3-5
20	200	0.05 (Ba)	212	0.06	364	4-8
21	200	0.125 (Ba)	211	0.13	351	3-4
22	200	0.25 (Ba)	215	0.26	353	2-3
23	200	0.50 (Ba)	221	0.50	345	2-6

<sup>a</sup>Synthesis condition: TPABr/SiO<sub>2</sub>= 0.1, OH<sup>-</sup>/ SiO<sub>2</sub>= 0.1, Temp.= 160 °C, Time= 16 h.<sup>b</sup>Determined by XRF.<sup>c</sup>Determined by the BET method.